Report for the Joint Use/Research of the Institute for Planetary Materials, Okayama University

30/05/2020

2019 fiscal year (project conducted Sept – Dec 2019)

Category: International Joint Research

Name of the research project: Ni isotope fractionation during Fe-oxide formation: implications for using Ni isotopes as a biomarker

Principal applicant: Madeleine Bohlin

Affiliated institution and department: Department of Earth Sciences, Uppsala University

Collaborators

Name: Ryoji Tanaka[1], Eizo Nakamura[1], Christoffer Hemmingsson[2], Anna Neubeck[3]

Affiliated institution and department: [1]Institute for Planetary Materials, Okayama University, [2]Department of Earth Sciences, Stockholm University, [3]Department of Earth Sciences, Uppsala University

1. Research purpose

Nickel (Ni), being a transition metal involved in the major marine redox cycles, as well as being a vital micronutrient used by both marine and terrestrial life, has enormous potential as a biogeochemical tracer. The ongoing project "Ni isotope fractionation during Fe-oxide formation: implications for using Ni isotopes as a biomarker" aims at constraining fundamental isotopic fractionation mechanisms and pathways during the formation of ferrihydrite, one of the most ubiquitous Fe-oxides on Earth. The results from the project will increase our understanding of the Ni isotopic system and help determine the capabilities of Ni isotopes as a geochemical tracer and biomarker.

1.1 Ni isotopes as a tracer of the causes and effects of the GOE

When ferrihydrite forms in the open ocean or in the marine sedimentary column, it incorporates a signal of the ambient seawater chemistry. Following this principle, the evolution of marine Ni concentrations during the great oxygenation event (GOE) approximately 2.4 Gyr ago, was reconstructed from the contemporaneous BIF record (Konhauser et al., 2009). The Ni concentration of BIFs, or banded iron formations, shows that Ni concentrations in the Archean ocean where up to 40 times higher than today, but that there was a steep and unidirectional decline as oxygen levels rose. The timing of a marked change in mantle dynamics and volcanism, a possible collapse in the methanogenic archaea community (which were and are, the primary Ni cycling organisms), the steep decline in marine Ni concentrations, and the increase in oxygen levels during the GOE has sparked intense debate on the importance and interaction of these events. A Ni isotopic record from this time window would greatly help in interpreting and understanding the sequence of events, and the role of changing sources, sinks and biological cycling of Ni at this crucial time in Earth's history. In the wake

of such a record, and in order to better interpret it, more knowledge needs to be accumulated about the fundamental principles of the Ni isotope system.

Several recent experimental studies have shown that adsorption of Ni onto ferrihydrite generally fractionate Ni isotopic compositions (reported as δ^{60}Ni = parts per thousand deviation of the ^{60}Ni/^{58}Ni ratio of a sample from the NIST SRM986 standard) of the solid by -0.34‰ from experimental fluids (Wasylenki et al., 2015; Wang and Wasylenki, 2017). However, these experiments are often conducted in low-ionic strength solutions containing only Fe and Ni. The Archean ocean had very high concentrations of silicon, Si, (up to 2.2 mM) as seen in the massive chert layers embedded within Archean BIFs. Konhauser et al., (2009) showed that the presence of Si greatly reduces the adsorption of Ni onto ferrihydrite, but so far no one has tested how Si affects the Ni isotopic compositions of the precipitating ferrihydrite crystals. If Si concentrations were indeed as high as 2.2 mM, it is likely that the very reduced incorporation of Ni into the oxides have large consequences for the resulting Ni isotopic composition.

1.2 Ni isotopes as a biomarker

Biological uptake and cycling of Ni is associated with large isotopic fractionations, were organisms preferentially retain the light isotopes. Laboratory-grown methanogenic archaea were shown to be between 0.44 to 1.5‰ lighter in their Ni isotopic composition relative to their growth medium (Cameron et al., 2009). These δ^{60}Ni values are considerably more negative than the composition of most terrestrial rocks (meteorites, basalts, loess, river sediments) with an average composition of +0.15±0.24‰ (Cameron et al., 2009). These findings sparked an interest in using the δ^{60}Ni composition of rock material to trace life where organic molecules may have been destroyed. This is of particular interest for tracing the origin of complex life on Earth and the search for extra-terrestrial life forms for future sample-return missions. However, before Ni isotopes can reliably be used as a biomarker several aspects of the system needs to be constrained. The most important question to answer is if purely abiotic reactions can fractionate Ni isotopes to similarly negative values as organisms can. So far, all experimental work involving Fe-oxides have been conducted in simple solutions, which although reveal the first-order controls on Ni isotope fractionation, do not provide a realistic view of what controls Ni isotopes in a natural environment. Much of the work on the earliest life on Earth has involved structures found in silica rich rocks (e.g. Djokic et al., 2017), and the search for extra-terrestrial life has found Earth-analogues in Si-rich hydrothermal sinter deposits (Ruff and Farmer, 2016). These findings make it abundantly clear that the impact of Si on Ni isotope fractionation is crucial to understand in order to use Ni isotopes as a reliable biogeochemical tracer in future work.

2. Conducted research

Extensive experimental work was conducted to study the sorption of Ni onto ferrihydrite under the presence of Si. The experimental strategy was designed to test the dependency of varying Ni concentrations, Si concentrations, mineral formation pH, and equilibration time on Ni and Si isotope fractionation during ferrihydrite formation. In addition, experiments were conducted as both coprecipitation and pure adsorption experiments. During coprecipitation experiments, Ni (and Si) was added to the experimental solution prior to ferrihydrite synthesis. As ferrihydrite precipitates, Ni and Si are incorporated into the ferrihydrite crystal structure, as well as adsorbed onto the surface. During adsorption experiments, ferrihydrite was synthesised prior to addition of Ni (and Si), either as pure ferrihydrite (adsorption experiment “A”) or ferrihydrite that had been precipitated together with Si (adsorption experiment “B”).

A total of 250 samples were collected from 125 experimental conditions. All samples were measured for elemental compositions via ICP-MS (inductively coupled mass spectrometry) and mineral determination was made via TEM (transmission electron microscopy) on a representative number of samples to ensure that ferrihydrite was synthesised. Further, the bonding environment between Ni, Si and ferrihydrite was investigated with Raman and infrared spectroscopy. These analyses were conducted by Chris Hemmingsson who is currently analysing that data, and it will therefore not be discussed further in this report. Due to time limitations, only 25 solid samples were analysed for Ni isotopes via MC-ICP-MS (multi collector inductively coupled mass spectrometry) at this stage. An additional 30 samples were analysed for Si isotopes by Chris Hemmingsson, some of which will be briefly discussed in this report.

2.1 Experimental procedure and strategy

All ferrihydrite synthesis experiments where conducted in high ionic strength solutions with seawater concentrations of NaCl of 0.5-0.6M and $Fe(II)Cl_2$ concentrations of 1mM. Ferrihydrite is precipitated by the gradual addition of 1M NaOH which oxides the ferrous iron. The NaOH was added at similar rates for all experiments (100uL every 10 seconds) and the increase in pH was noted down in order to control the effects of precipitation rates. The experimental solutions were taken to the target pH (7 for experiments 1 and 2, and ranging between 4 and 9 for experiment 4) and left to equilibrate for 30 min before collecting the samples. During this stage, 0.1M NaOH and/or 0.1M HCl was added as needed to keep the pH within 0.1 pH units of the target.

Stock solutions of HCl, $Fe(II)Cl_2$, Si and Ni where made prior to commencing the first experiments. The same stock solutions where used for all experiments. Stock solutions of NaCl and NaOH where made at more regular intervals and new batches where noted down for each experiment.

The experimental strategy was designed to test the dependency of varying Ni concentrations (experiment 1), Si concentrations (experiments 1 and 4), mineral formation pH (experiments 3 and 4) and equilibration time (experiment 2) on Ni and Si isotope compositions of ferrihydrite crystals. In addition, experiments where conducted as both coprecipitation and pure adsorption experiments as described below.

Experiments labelled "C" - Coprecipitation of Ni and Si: Ferrihydrite is precipitated in a solution containing Ni and Si. These elements will therefore be both incorporated into the mineral structure and adsorbed onto mineral surfaces.

Experiments labelled "A" – Adsorption onto pure mineral: A two-step experimental procedure was conducted where pure ferrihydrite is initially precipitated at pH 7.5 in the NaCl solution (i.e. no Ni or Si present). The mineral is then separated from the solution via centrifugation, and a new NaCl solution containing Ni and Si is added. This experiment studies the behaviour during adsorption of Ni and Si onto the mineral surface without the influence of these elements within the mineral lattice.

Experiments labelled "B" – Adsorption onto Si-containing mineral: The initial ferrihydrite mineral is formed with Si present (NaCl, Fe and Si), and Ni and Si are then let to adsorb onto the surface in a second step. The initial presence of Si in the ferrihydrite structure is predicted to significantly change the surface charge of the mineral and hence the adsorption characteristics of both Ni and Si, and hence their isotopic fractionation.

The coprecipitation and adsorption experiments were performed in four different experiments (experiments 1-4) described below.

2.1.1 Experiment 1: Varying Ni and Si concentrations

Ranging Ni concentrations (200-4000 nM Ni) for 4 different Si concentrations (0, 0.67, 1.1 and 2.2 mM). Experiment 1 is designed to test the previously published elemental partition coefficient of Ni into ferrihydrite under the influence of Si in the solution (Konhauser et al., 2009), and provide new isotopic fractionation factors. A total of 132 samples (66 solids and 66 fluids) where collected for experiment 1.

2.1.2 Experiment 2: Time series

Experiment 2 was designed to test the time scale and potential kinetic effects on Si and Ni elemental partitioning and isotopic equilibrium. The standard NaCl and $Fe(II)Cl_2$ concentrations where used (0.6M and 1mM respectively) with 2500nM Ni and 2.2mM Si to ensure high enough concentrations for isotopic measurements. The experiment was run as a coprecipitation experiment ("C"). 11 samples were collected between 0 and 96 hours.

2.1.3 Experiment 3: pH dependency prior to time series

3 samples were collected during the rapid increase in pH prior to stabilising at pH 7 for the time series sampling (pH 4, 5 and 6). The compositions of these samples will be compared to those of Experiment 4 where the forming solids where equilibrated for 30 minutes (estimated "equilibration" time was a couple of minutes for these samples).

2.1.4 Experiment 4: pH dependency

Ferrihydrite was synthesised and stabilised for 30 minutes at a range of pH values (4, 5, 6, 7, 8, 9). A solution with standard NaCl and $Fe(II)Cl_2$ concentrations where used (0.6M and 1mM respectively) with a Ni concentration of 2500 nM. As in experiment 1, different Si concentrations where used (0, 1.1 and 2.2 mM) and both co-precipitation and adsorption experiments where conducted (C, A, B). The experiment was designed to further test and separate the effects of Ni and Si incorporation vs surface adsorption, as more Ni is adsorbed at high pH (<7), increasing the proportion of structurally incorporated Ni at lower pH ranges (Wang and Wasylenki, 2017). A total of 96 samples (48 solids and 48 fluids) where collected for Experiment 4.

2.2 Element analysis using ICP-MS

Samples were analysed for Fe, Na, Ni and Si concentrations on the ElementXR Inductively Coupled Mass Spectrometer (ICP-MS) in medium and high resolutions. A PFA double pass spray chamber with a peltier cooler at 4 degrees was used, together with a 50 uL/min PFA nebulizer and Ni-H and Ni-normal cones.

Separate calibration standards were made for each type of sample (Solid, Fluid, Initial fluid) to ensure a fully matrix matched calibration. Every 7 samples where bracketed with a standard (typically a dilution of the calibration standard) to correct for drift during the analytical sequence. Blank correction was made by subtracting the average signal of the acid blanks preceding and following the sample brackets, assuming a linear evolution between blanks. To ensure reproducibility, internal standards were made from each sample category and analysed several times throughout each analytical session.

2.3 Separation of Ni using column chromatography

2.3.1 Spiking of samples

A double spike method was used where a ^{61}Ni-^{62}Ni spike (containing equal proportions of ^{61}Ni and ^{62}Ni) was added to all samples prior to chemical processing. The double spike allows correction of

instrumental mass bias occurring during analysis as well as possible fractionation arising from less than 100% yields during column chromatography. Samples and standards containing 200 ng Ni were transferred to precleaned PFA vials. The spike was then added at a Ni_{sample}/Ni_{spike} ratio of 1 and evaporated to dryness in a series of steps. Firstly, a few drops of concentrated HF were added to the sample/spike solution and evaporated on a hotplate at ~110°C to remove the silicon in the sample. When dry, 10 drops of 6M single distilled HCl was added and again evaporated, converting any residual nitrate salts from the spike solution into chloride salts. Following evaporation, 1 ml 6M single distilled HCl was added and left to reflux for a few hours on the hotplate to ensure that the sample/spike mixture was completely dissolved and homogenised. The mixture was then taken off the hotplate and left in room temperature to cool down before loading it onto the first anion column. Each batch of samples included a minimum of 2 certified rock standards with known Ni isotopic compositions (BHVO-2, PCC-1) to ensure analytical accuracy.

2.3.2 Anion column: Removal of Fe

The first column step follows that of Yamakawa et al., (2009) and utilises the AG1-X8 anion exchange resin to separate Ni from Fe. The resin was added to 1ml plastic columns with a 9 ml reservoir. To remove contaminant elements the resin was first cleaned with 9 ml 0.5M HCl, 9 ml 3M HNO_3, 9 ml 0.5M HCl, 9 ml 8M HNO_3, 18 ml MilliQ water and lastly 12 ml 6M HCl. Following cleaning, the resin was conditioned using 5 ml 6M single distilled HCl. The samples were then loaded onto the columns and Ni was eluted with an additional 4ml 6M single distilled HCl. The samples, which were collected into precleaned PFA vials, were subsequently dried down on a hot plate at ~110°C.

2.3.3 Ni Eichrome resin column

The anion resin removes most of the Fe from the sample, but other matrix elements such as Na and Si coelute with Ni, and these and remnant amounts of Fe need to be further separated using a Ni specific resin. The Ni-spec Eichrome resin contains a dimethylglyoxime (DMG) molecule, which at pH >8 forms a Ni-DMG complex which is strongly retained in the resin. The dry sample-spike residues were dissolved in 1 ml 0.5M HCl and placed on a hotplate for about 30 to 60 minutes to ensure complete dissolution. After dissolution the pH of the sample was increased to ~9 by the addition of 0.3 ml 1M ammonium citrate and 0.2 ml concentrated ammonia (NH_3).

Approximately 0.3 ml wet Ni-spec resin was loaded into polypropylene columns. The resin was washed with 3 ml MilliQ water and 1.5 ml of 0.2M ammonium citrate to wash out potential contaminant elements. The resin was then conditioned with 3 ml 0.2M ammonium citrate + NH_3 to buffer the resin pH to 9. The prepared sample solution was then loaded onto the column and let to equilibrate for 1 h.

After 1 hour the columns were washed with 6 ml of the 0.2M ammonium citrate+NH_3 solution, washing out the sample matrix elements (Na and remnant Fe and Si). Thereafter, 6 ml of MilliQ water was added to wash out excess ammonium citrate and ammonia salts. Ni was then collected in 4 ml of 3M HNO_3. The collected Ni cuts were then dried down on a hot plate at ~100°C overnight.

2.3.4 Post-column sample processing

Following separation through the Ni specific resin and evaporation, the sample is refluxed in 0.5 ml aqua regia for 24 hours at ~120°C. This breaks down organic compounds generated from the resin which may cause interferences during mass spectrometric analysis. After refluxing, the samples were dried down, and 5 drops of concentrated single distilled HNO_3 was added and again dried down, to fully remove traces of chloride salts. When the sample was dry, 1 ml of 0.5M HNO_3 was added and

the sample was refluxed for ~1hour on a hotplate to ensure that the sample was fully dissolved and ready for isotopic analysis.

2.4 Ni isotope analysis using MC-ICP-MS

Ni isotopes were analysed on the NeptunePLUS multi-collector inductively coupled plasma mass spectrometer (MC-ICP-MS) using an Aridus desolvator introduction system, 50uL/min ESI nebuliser, 1.8mm platinum injector, and Ni-H and Ni-X cones. Typical sensitivity for ^{58}Ni in medium resolution was 10V for ~80ppb. The analyses were made in medium resolution with simultaneous measurements of ^{58}Ni, ^{60}Ni, ^{61}Ni, ^{62}Ni and ^{64}Ni, as well as ^{56}Fe to monitor the isobaric interference of ^{58}Fe on ^{58}Ni. Each sample was measured with 25 cycles of 8 seconds integration time and was separated by acid blank measurements and measurements of the NIST SRM986 standard every 2 samples. Every analytical sequence started and finished with the measurement of two inhouse instrumental standards (Ni-Romil and Ni-Wako) to monitor the reproducibility and daily performance of the instrument.

2.5 Data reduction scheme

The data reduction is based on double spike calculations by Rudge et al., (2009). An excel spread sheet containing the calculation matrices was provided by Ryoji Tanaka and used for all data reduction.

Nickel isotope compositions of samples are expressed using the delta (δ) notation where the isotopic ratio of the sample is normalised to that of the NIST SRM 986 standard, following:

$$\delta^{X}Ni_{sample}\ (‰) = \left(\frac{{}^{X}Ni/{}^{58}Ni_{Sample}}{{}^{X}Ni/{}^{58}Ni_{NIST\ SRM\ 986}} - 1\right) \times 1000$$

where X denotes either the ^{60}Ni, ^{61}Ni or ^{62}Ni isotope (^{64}Ni was not considered in this study). The data presented in this study is described using the ^{60}Ni/^{58}Ni ratio given as δ^{60}Ni. Prior to double spike calculation, the ^{58}Ni intensity was corrected for interference of ^{58}Fe following:

$${}^{58}Fe = {}^{56}Fe_{Measured} \times \left(\frac{{}^{58}Fe}{{}^{56}Fe}\right)_{Natural}$$

where ^{58}Fe/^{56}Fe$_{natural}$ is the ratio of the natural abundances of the ^{58}Fe and ^{56}Fe isotopes. The intensity of ^{58}Fe is then subtracted from the measured ^{58}Ni signal.

3. Research outcomes

3.0.1 Reproducibility of experiments and accuracy of data

A total of 250 solid and fluid samples were collected from 125 experimental conditions. Some experiments were duplicated allowing the reproducibility of the experimental setup to be assessed. Ni/Fe ratios and δ^{60}Ni values of experimental solids with the same initial setup (e.g. 1C17, 2C2, 4C4) are identical compared to the range observed throughout the experiments (Ni/Fe of 0.001±0.0001 and d60Ni of -0.353±0.073‰). Si/Fe and δ^{30}Si however are much more variable (Si/Fe of 1.33±1.16 and δ^{30}Si of 0.39±0.48‰ for the same set of experiments as for Ni above). The stability of the behaviour of Ni compared to the very unstable behaviour of Si is also observed in the time-series experiment (experiment 2) and discussed further below.

The accuracy and reproducibility of the Ni isotopic data was assessed based on the repeated measurements of both certified rock standards and inhouse Ni standards. Instrumental reproducibility between the analytical sessions was determined by repeated measurements of the inhouse Ni monoelemental standards "Ni Wako", which yielded a value of -0.206 ± 0.077 ‰, (n=19) and "Ni Romil" yielding a value of 0.027±0.050‰ (n=7). These are in good agreement with measurements made in 2018 where Ni Wako was measured as -0.176±0.055‰ (n =11). The accuracy and full reproducibility of the full chemical and analytical procedure was assessed by the repeated column processing and analysis of the Wako standard and the BHVO2 and PCC1 rock standards with known Ni isotopic compositions. Ni Wako was passed through the columns 6 times yielding a value of -0.203±0.102‰, in excellent agreement with its previously measured value. BHVO2 yielded a value of 0.090±0.08‰ (n=1), in good agreement with published values and values obtained previously by this project in 2018 (0.023±0.052, n=9), and PCC1 yielded values of 0.180±0.044 (n=3) in good agreement with published values and those obtained in 2018 (0.168±0.057‰, n=5).

3.1 Experiment 1

3.1.1 Ni partitioning behaviour during coprecipitation and adsorption

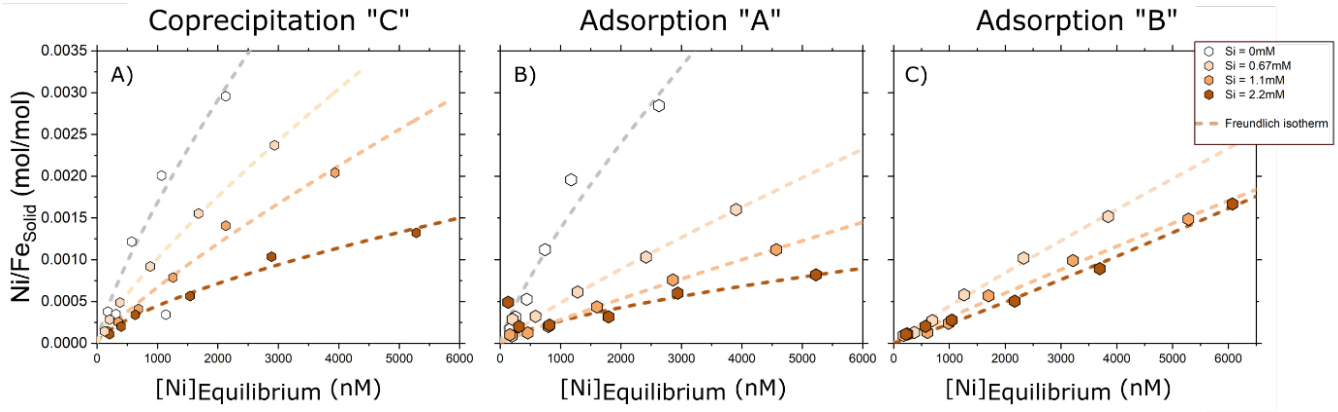

Figure 1 – Ni/Fe ratios in ferrihydrite solids showing the dependency of experimental Ni and Si concentrations for A) coprecipitation, B) adsorption onto pure ferrihydrite, and C) adsorption onto ferrihydrite already containing Si. The Ni-equilibration concentration (x-axis) is the concentration in the experimental fluid following mineral synthesis. The ferrihydrite solids increase in Ni/Fe with increasing Ni concentration in the experiment, however the increase is non-linear suggesting a saturation behaviour. Higher Si concentrations in the experiments likely lead to higher competition between Ni and Si for surface sites, and solids reach saturation for Ni more rapidly (resulting in lower Ni/Fe). This behaviour is seen for all experimental conditions. The data is modelled with Freundlich adsorption isotherms which allow the quantification of adsorption characteristics and a quantitative comparison of sorption mechanisms.

Experiment 1 was designed to test the partitioning behaviour of Ni and the associated isotopic fractionation during coprecipitation and adsorption onto ferrihydrite. Ni concentrations ranged between 200-4000 nM and Si concentrations were fixed at either 0, 0.67, 1.1 or 2.2 mM. The Ni/Fe ratio of the ferrihydrite solids increases nearly linearly with increasing Ni concentration in the experiment, suggesting a near constant partition coefficient of Ni at these concentrations (fig 1; table 1). The deviation from a perfect linear relationship however suggest a degree of saturation of the sorption capacity. This saturation is reached faster where more Si in involved (fig 1). Higher concentrations of Si systematically lower the fraction of Ni incorporated or adsorbed on the solids, in good agreement with previous studies (Konhauser et al., 2009). Higher Si concentrations in the experiments likely lead to higher competition between Ni and Si for surface sites, and solids reach saturation for Ni more rapidly (resulting in lower Ni/Fe and less linear trends). This behaviour is observed for all sorption mechanisms, i.e. for coprecipitation, adsorption onto pure ferrihydrite and adsorption onto ferrihydrite containing Si. Coprecipitation however leads to higher Ni/Fe ratios for

any given Ni and Si concentration, compared to both the adsorption experiments (fig 2). This is expected since the coprecipitated solids have Ni which is both incorporated structurally and adsorbed onto the surface of the ferrihydrite crystals.

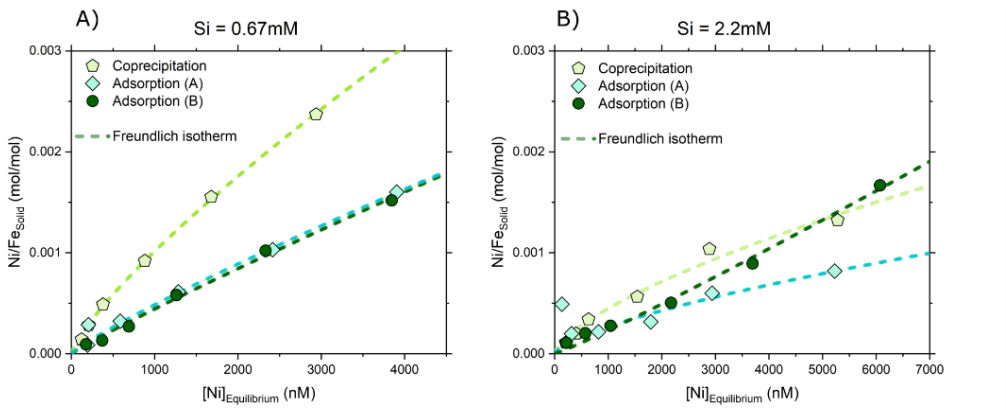

Figure 2 - Ni/Fe ratio in solids showing the effects of changing Ni sorption mechanism for A) a Si concentration of 0.67mM, and B) a Si concentration of 2.2mM. Coprecipitation leads to more incorporation of Ni compared to adsorption (both type A and B), however this difference is less pronounced at higher Si concentrations. As in figure 1, the dashed lines represent best-fit of Freundlich adsorption isotherms to the data.

3.1.2 Ni isotopic fractionation during coprecipitation and adsorption

Due to time limitations at the end of the project duration in 2019, only 25 solid samples have so far been analysed for their Ni isotopic composition. However, the results obtained indicate that Si concentrations, in combination with sorption mechanism, play a crucial role in the resulting Ni isotopic composition of the ferrihydrite (fig 3).

The Ni isotopic compositions of the ferrihydrite solids were all isotopically lighter than the starting fluid composition (~-0.2‰) and ranged from -0.86 to -0.22‰ (table 1). δ^{60}Ni of the solids increase towards the initial fluid composition as the fraction of Ni incorporated in the solids increases, and they are lowest when very little Ni is incorporated (fig 3). Although fluid samples have not yet been analysed, based on mass balance and the results from previous studies (e.g. Wang and Wasylenki, 2017; Wasylenki et al., 2015; Gueguen et al., 2018;Neubeck et al., in prep) they are expected to be isotopically heavier than the solids and the starting fluid composition. The Ni isotopic composition of the coprecipitated and adsorbed solids not containing Si have δ^{60}Ni values and fractionation behaviours in agreement with previous coprecipitation and adsorption experiments (fig 3; Wasylenki et al., 2015; Wang and Wasylenki, 2017). However, when Si is present in the experimental fluids at 2.2 mM the solids become isotopically lighter. The greatest difference is observed during pure adsorption, with samples being twice as fractionated as when Si is not present (fig 3). The samples can be modelled by both batch equilibrium fractionation and Rayleigh fractionation; more data from the residual solid and fluid samples is needed to establish the mechanism of fractionation and if there is a difference between the incorporation mechanisms or Si concentrations.

These results have implications for the use of Ni isotopes as a biomarker. Lab grown methanogenic archaea where shown to range -0.44 to -1.5‰ (average -0.7‰) from their growth medium, which is distinctly more negative than most crustal rocks with values around +0.15‰ (Cameron et al., 2009). However, the very negative δ^{60}Ni values obtained in these purely abiotic experiments, through adsorption of Ni onto ferrihydrite in the presence of Si, directly overlaps with this 'biogenic signal'. Given that signs of early lifeforms, or hypothesised extra-terrestrial lifeforms, are often associated

with high-Si deposits (Ruff and Farmer, 2016; Djokic et al., 2017) it will be crucial to establish the detailed controls on Ni isotope fractionation in these high Si systems, in order to reliably use Ni isotopes as a biomarker in future work.

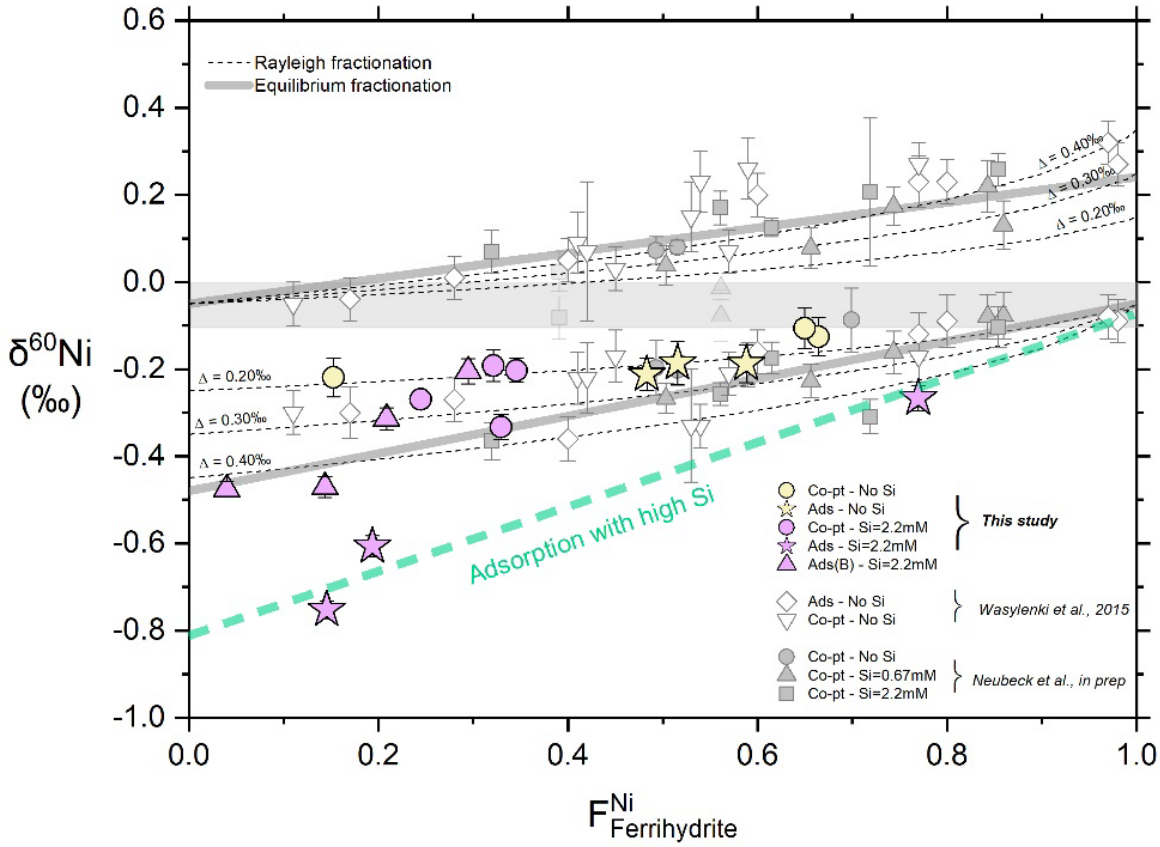

Figure 3 – Ni isotopic composition (δ^{60}Ni) against fraction of Ni sorbed to Ferrihydrite ($F^{Ni}_{Ferrihydrite}$) from Experiment 1. Yellow samples do not contain Si while pink samples where synthesised with 2.2mM Si. The grey box is the composition of the initial experimental fluid, grey solid lines are best fit equilibrium batch fractionation of fluid and solids from previously published studies (with a fractionation of -0.34‰), and the dashed lines are Rayleigh fractionation lines for different fractionation factors ranging from -0.2 to -0.4‰. Non-Si samples fall on top of previously published values for similar experiments. Although coprecipitation samples with Si roughly follow the same fractionation line as previous studies, the adsorption experiments show much more negative δ^{60}Ni values, with a suggested isotopic fractionation of -0.8‰. Isotopic analyses of experimental fluids are crucial in determining this value. Reference data from Wasylenki et al. (2015) and Neubeck et al. (in prep).

3.2 Experiment 2 and 3

Experiment 2 was designed to test the equilibrium time scale of the Ni partitioning and isotopic fractionation during precipitation of ferrihydrite. Previous results from measurements of Si isotopes in a similar experimental setup suggested that although elemental equilibrium was reached, Si isotopic equilibrium was never reached in the time frame of the experiment (72h; Chris Hemmingsson, unpublished data). If this is true also for Ni, it would have large implications for the interpretation of a geological archive of Ni isotopes. To test the timescale of Ni elemental and isotope equilibrium and test the potential co-variation between Ni and Si with time, Experiment 2 was run as a coprecipitation experiment for 96 hours. 3 samples were also collected during the rise in pH (Experiment 3) and these results will later be compared to those of Experiment 4 were samples were equilibrated for 30 min at the same pH (4, 5 and 6).

3.2.1 Ni partitioning behaviour with time

Ni/Fe ratios of the ferrihydrite solids reached equilibrium within the first hour of the experiment (fig 4a; table 2). Apart from the first sample at time 0 where Ni/Fe ratios are higher (i.e. the experiment solution had just reached a pH of 7 and no time was left for equilibration), all following samples have a constant value for the remainder of the experiment. The Ni/Fe ratio is identical to samples 1C17 and 4C4 which have the same initial conditions, but were equilibrated for only 0.5 hours, suggesting that the equilibration time for Ni partitioning, at least during coprecipitation, is less than 30 minutes.

Si elemental partitioning reaches equilibrium during the first hour of the experiment, with Si/Fe ratios only fluctuating slightly within the first hour (fig 4b). As the pH is increased from approximately 2 to 7 before the time series is started, the fraction of Ni that is sorbed steadily increases, and the value approaches the ratio of the initial fluid as pH reaches 7. However, that value is rapidly lowered as the pH stabilised. Si on the other hand fluctuates more unpredictably during the pH rise, suggesting a more complex control on the partitioning of Si compared to Ni.

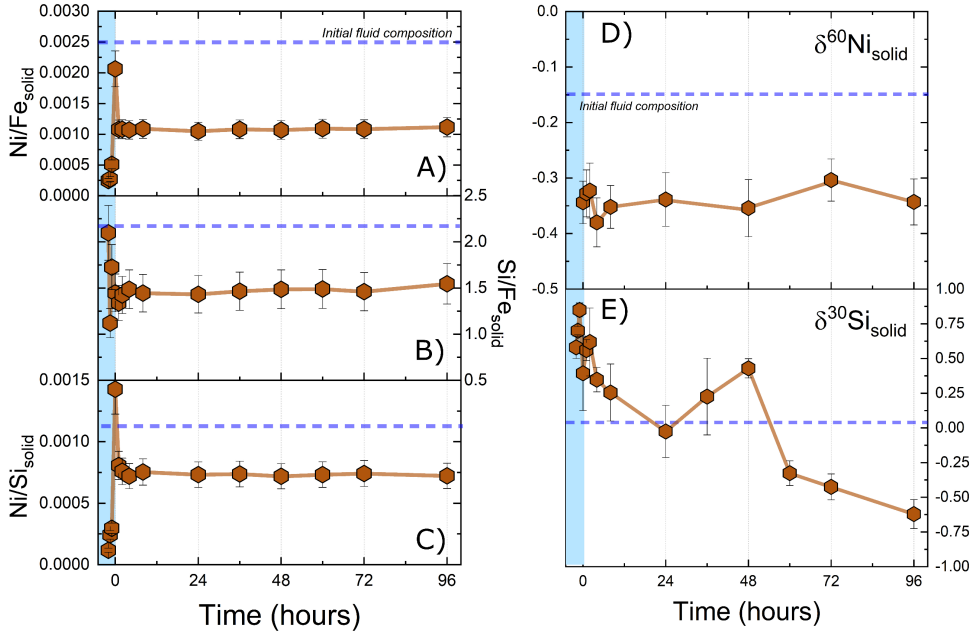

Figure 4 – Variations in A) Ni/Fe, B) Si/Fe, C) Ni/Si, D) Ni isotopic composition and E) Si isotopic composition of solid ferrihydrite with time. All element ratios are expressed in mol/mol. δ^{60}Ni and δ^{30}Si are expressed in ‰. Ni and Si rapidly reach elemental equilibrium, and Ni reach isotopic equilibrium immediately during the experiment. Si isotopes on the other hand show a more complex behaviour with decreasing δ30Si as time progresses. Si does not reach isotopic equilibrium during the first 96 hours.

3.2.2 Ni isotopic fractionation with time

The Ni isotopic composition of the ferrihydrite solids rapidly reach equilibrium, on similar time scales as the elemental Ni/Fe partitioning (fig 4d). Further, the value of -0.34±0.04‰ (2σ, all 9 samples) is identical within error of experiment 1C17 which had the same experimental setup, but much shorter equilibration time (30 min). These results have important implications for future interpretations of geological archives. The fast equilibration times with stable and predictable Ni/Fe and Ni isotope ratios are encouraging as it suggests the Ni system is robust with a few, predictable controls. This is in stark contrast to the Si isotopic system which display a much more complex behaviour (fig 4e).

δ^{30}Si values initially increase steadily at very positive values (approaching +1‰) during the initial rise in pH and fluctuates at positive values during the first 2 hours, before steadily decreasing to very negative values (approaching -0.75‰) throughout the remainder of the experiment. The Si isotopic composition of the ferrihydrites do not reach isotopic equilibrium during the 96 hours the experiment was conducted, despite an almost immediate elemental equilibrium. This suggests that Si isotopes have a more complex behaviour than Ni isotopes, possibly controlled by reaction kinetics and variations in Si speciation or complexation during the experiment, which favours more and more light Si isotopes to be adsorbed and/or incorporated. Comparing the results from Experiment 2 with those of 1C17, where δ^{30}Si was 0.22‰ after 0.5h of equilibration, whereas in experiment 2 the value at that equilibration time is ~0.5‰, suggests that Si isotopes are more unpredictable and are not easily reproducible between the experiments. Further isotopic analyses coupled to data on bonding environment from Raman and infrared spectrometry will be crucial in determining the controls on Si isotope fractionation in these conditions. However, the disequilibrium in δ^{30}Si and the variations in the control on Si isotope fractionation does not appear to affect Ni isotopes.

3.3 Experiment 4

Experiment 4 was designed to test the pH dependency of Ni elemental partitioning and associated Ni isotope fractionation. It further aims to separate the potential effects and differences between coprecipitation and adsorption. The relationship between adsorption and structurally incorporated Ni during coprecipitation is believed to be pH dependent, as adsorption is more sensitive to pH and becomes more important at high pH. This means that the fraction of structural incorporation is relatively higher at lower pH (Wang and Wasylenki, 2017).

3.3.1 Ni partitioning behaviour with varying pH

At low pH the fraction of Ni that is incorporated and adsorbed to the ferrihydrite is small, with a minimum value of 0.004 (i.e. 0.4% of Ni in the experiment is incorporated into the solid phase). Ni/Fe ratios remain low until pH reaches 7, after which the sorption increases rapidly to close to 100% (maximum incorporation in these experiments was 98%), with solid Ni/Fe approaching those of the initial fluid at pH 8 and 9 (fig 5). The coprecipitation experiments have higher Ni/Fe ratios at low pH compared to the adsorption experiments, an effect which is more pronounced when Si is present in the experimental fluid (fig 5). This suggests that the presence of Si has a larger effect on adsorption of Ni compared to when it is structurally incorporated. This is in agreement which the isotopic data from Experiment 1 which showed that Si has the largest effect on adsorbed Ni isotope values.

The Si/Fe ratio on the other hand is unaffected by the change in pH and has a constant partition behaviour into the ferrihydrite (fig 5h). There is however a large difference between the incorporation mechanisms with coprecipitation leading to much higher Si concentrations compared to adsorption onto pure ferrihydrite. Interestingly, when Si is incorporated into the ferrihydrite prior to additional adsorption of Ni and Si (i.e. adsorption “B”), the Si/Fe ratios following the additional adsorption do not reach higher values than for coprecipitation. This suggests that the mineral surfaces are completely saturated with respect to Si, not allowing more Si to adsorb onto the ferrihydrite surface. This Si saturation does however not have as pronounced effect on Ni, which still adsorbs despite Si saturation with similar Ni/Fe ratios for adsorption “A” and “B”. This suggest that the competition between Si and Ni is only effective to a certain degree as Si may become saturated faster than Ni (at least at these high concentrations).

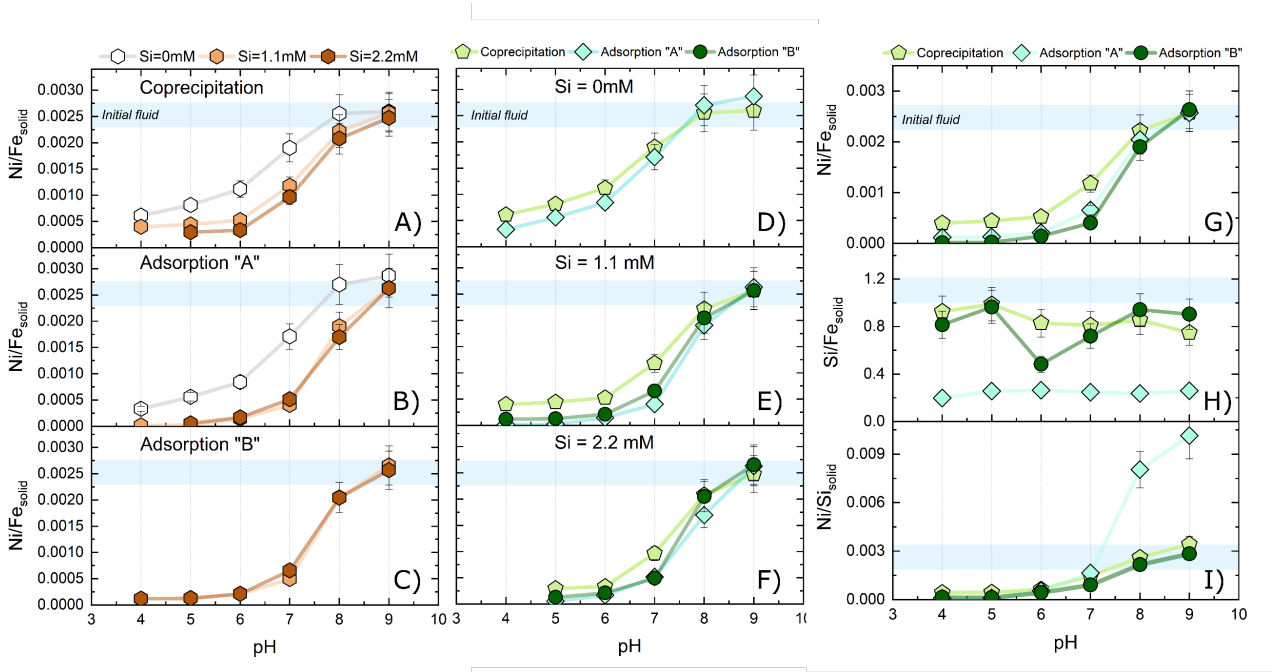

Figure 5 – Variations in ferrihydrite solid Ni/Fe ratio with pH and varying Si concentrations for A) coprecipitation, B) adsorption onto pure ferrihydrite and C) adsorption onto ferrihydrite containing Si. Panels D-F show the variations in Ni/Fe for the different incorporation mechanisms for each Si concentrations of D) 0 mM, E) 1.1 mM and F) 2.2mM. Panels G-I all have the same Si concentration of 1.1mM and show the variations in G) Ni/Fe, H) Si/Fe and I) Ni/Si of the solids. All element ratios are given as molar ratios (mol/mol). See text for discussion.

3.3.2 Ni isotopic fractionation with varying pH

The solids and fluids from Experiment 4 have not yet been analysed for their Ni isotopic composition, but based on the larger range in Ni/Fe ratios (and thus the fraction of Ni incorporated into the solids), these are expected to vary more than the solids analysed so far in experiment 1. Further, the relationship between structurally incorporated and adsorbed Ni is expected to generate a large difference, as incorporated Ni is hypothesised to have a heavier isotopic composition than surface adsorbed Ni (Wang and Wasylenki, 2017), implying that solids precipitated at low pH may have higher δ^{60}Ni values.

4. Implications

The results obtained thus far from the adsorption and co-precipitation experiments conducted in 2019 reveals critical information on the controls on both present-day geochemical cycling of Ni, as well as for reconstructing past seawater compositions on Earth from the δ^{60}Ni composition of sedimentary archives. Adsorption experiments in a high ionic strength fluid mimics the scavenging of Ni of settling ferrihydrite solids (which is a common continental weathering product) in the oceanic water column. Coprecipitation experiments on the other hand mimics precipitation of ferrihydrite at the oxic-anoxic interface in the marine sedimentary column, where Ni is incorporated into the structure of oxides. Both these processes are believed to exert a strong control on Ni in the modern and past ocean, but the isotopic fractionation factors are not well constrained, as seen in the current enormous gaps in the modern oceanic Ni and δ^{60}Ni budgets (e.g. Gall et al., 2013; Vance et al., 2016). The results from this study sheds light on these key processes and puts constraints on the controlling mechanisms of Ni isotope fractionation, especially in more complex experimental conditions with high ionic strength and high Si concentrations, making it possible to investigate causes and effects of varying δ^{60}Ni in our geological past. Further, the knowledge obtained from this study will establish how reliable Ni isotopes are as a biomarker, which is crucial in the preparation phase of future sample-

return missions, where extra-terrestrial material is brought back to Earth to investigate the existence of life outside our planet.

5. Future research

To finalise the project, Ni isotope analyses will be conducted on the remaining samples. Importantly, the fluid samples need to be analysed in order to properly quantify isotopic fractionation factors. Samples of the initial experimental fluids and solids collected following the initial precipitation of ferrihydrite for both the adsorption experiments (A and B) will be analysed for their Ni/Fe ratios. This will allow the calculation of a mass balance which is crucial for quantitatively comparing and determining the differences between coprecipitation and adsorption, when Si is present in the initial structure. Further, the mineral bonding environment data collected in 2019 by Chris Hemmingsson for this project will be analysed and interpreted. This is important in order to understand the mechanistic reason for isotope fractionation. This is particularly important for determining the reason Ni isotopes are more fractionated during adsorption with Si compared to coprecipitation.

6. References

Cameron, V., Vance, D., Archer, C. and House, C. H. (2009) A biomarker based on the stable isotopes of nickel, Proceedings of the National Academy of Sciences 106, 10944-10948

Djokic, T., Van Kranendonk, M. J., Campbell, K. A., Walter, M. R., Ward, C. R. (2017) Earliest signs of life on land preserved in ca. 3.5 Ga hot spring deposits, Nature Communications 8, 15263

Gall, L., Williams, H. M., Siebert, C., Halliday, A. N., Herrington, R. J. and Hein, J. R. (2013) Nickel isotopic compositions of ferromanganese crusts and the constancy of deep ocean inputs and continental weathering effects over the Cenozoic, Earth and Planetary Science Letters 375, 148-155

Gueguen, B., Sorensen, J. V., Lalonde, S. V., Peña, J., Toner, B. M. (2018) variable Ni isotope fractionation between Fe-oxyhydroxides and implications for the use of Ni isotopes as geochemical tracers, Chemical Geology 481, 38-52

Konhauser, K. O., Pecoits, E., Lalonde, S. V., Papineau, D., Nisbet, E. G., Barley, M. E., Arndt, N. T., Zahnle, K. and Kamber, B. (2009) Oceanic nickel depletion and a methanogen famine before the Great Oxidation Event, Nature 458, 750-754

Neubeck, A., Hemmingsson, C., Bohlin, M., Boosman, A., Rouxel, O., Ni isotope fractionation during coprecipitation of Fe(III)(oxyhydr)oxides in Si solutions, in prep

Rudge, J. F., Reynolds, B. C., Bourdon, B. (2009) the doubke spike toolbox, Chemical geology 265, 420-431

Ruff, S. W., and Farmer, J. D. (2016) Silica deposits on Mars with features resembling hot spring biosignatures at El Tatio in Chile, Nature Communications 7, 13554

Vance, D., Little, S. H., Archer, C., Cameron, V., Andersen, M. B., Rijkenberg, M. J. A. and Lyons, T. W. (2016) The oceanic budget of nickel and zinc isotopes: the importance of sulfidic environments as illustrated by the Black Sea, Philosophical Transactions of the Royal Society A 374

Wang, S-J. and Wasylenki, L. E. (2017) Experimental constraints on reconstruction of Archean seawater Ni isotopic composition from banded iron formations, Geochimica et Cosmochimica Acta 206, 137-150

Wasylenki, L. E., Howe, H., D., Spivak-Birndorf, L. J. and Bish, D. L. (2015) Ni isotope fractionation during sorption to ferrihydrite: Implications for Ni in banded iron formations, Chemical Geology 400, 56-64

Yamakawa, A., Yamashita, K., Makishima, A., Nakamura, E. (2009) Chemical separation and mass spectrometry of Cr, Fe, Ni, Zn and Cu in terrestrial and extraterrestrial materials using thermal ionization mass spectrometry, Analytical Chemistry 81, 9787-9794

Table 1 – Chemical data for ferrihydrite solids and experimental fluids from Experiment 1

	Initial fluid		Solids							Fluids					
Sample ID	**Si initial**	**Ni initial**	**Ni/Fe**	**Ni/Si**	**Si/Fe**	**δ^{60}Ni**	**2se**	**δ^{30}Si**	**2σ**	**Ni/Fe**	**Ni/Si**	**Si/Fe**	**F^{Ni}_{Solid}**	**F^{Fe}_{Solid}**	**F^{Si}_{Solid}**
	mM	*nM*	*mol/mol*	*mol/mol*	*mol/mol*	*‰*	*‰*	*‰*	*‰*	*mol/mol*	*mol/mol*	*mol/mol*			
Coprecipitation															
1C1	0	200	0.0004			-0.235	0.043			0.016			0.66	0.99	
1C2	0	400	0.0004							0.031			0.51	0.99	
1C3	0	700	0.0003			-0.329	0.045			0.002			0.15	0.45	
1C4	0	1400	0.0012							0.033			0.68	0.98	
1C5	0	2500	0.0020			-0.216	0.047			0.175			0.65	0.99	
1C6	0	4000	0.0030							0.405			0.56	0.99	
1C19	0.67	200	0.0001	0.0002	0.64					0.020	0.001	0.020	0.53	0.99	0.73
1C20	0.67	400	0.0003	0.0005	0.62					0.040	0.001	0.040	0.56	0.99	0.75
1C21	0.67	700	0.0005	0.0008	0.63					0.182	0.002	0.182	0.55	1.00	0.74
1C22	0.67	1400	0.0009	0.0015	0.63					0.418	0.005	0.418	0.48	1.00	0.75
1C23	0.67	2500	0.0016	0.0025	0.63					1.328	0.008	1.328	0.47	1.00	0.74
1C24	0.67	4000	0.0024	0.0037	0.63					2.950	0.013	2.950	0.45	1.00	0.74
1C7	1.1	200	0.0001	0.0001	0.95					0.154	0.000	0.154	0.42	1.00	0.66
1C8	1.1	400	0.0003	0.0003	1.01					0.050	0.001	0.050	0.40	0.99	0.71
1C9	1.1	700	0.0004	0.0004	1.01					0.471	0.002	0.471	0.35	1.00	0.72
1C10	1.1	1400	0.0008	0.0008	1.03					0.832	0.003	0.832	0.37	1.00	0.72
1C11	1.1	2500	0.0014	0.0014	1.01					3.322	0.005	3.322	0.38	1.00	0.71
1C12	1.1	4000	0.0020	0.0020	1.03					3.846	0.010	3.846	0.33	1.00	0.72
1C13	2.2	200	0.0001	0.0001	1.67	-0.443	0.029	0.50	0.04	0.046	0.000	0.046	0.33	1.00	0.59
1C14	2.2	400	0.0002	0.0001	1.81	-0.302	0.036	0.98	0.04	0.149	0.000	0.149	0.32	1.00	0.64
1C15	2.2	700	0.0003	0.0002	1.70	-0.313	0.028	0.64	0.19	0.253	0.001	0.253	0.35	1.00	0.64
1C16	2.2	1400	0.0006	0.0003	1.86			0.78	0.05	0.746	0.002	0.746	0.26	1.00	0.68
1C17	2.2	2500	0.0010	0.0005	1.90	-0.379	0.022	0.22	0.10	1.047	0.003	1.047	0.24	1.00	0.66
1C18	2.2	4000	0.0013	0.0007	1.93			0.01	0.06	0.536	0.006	0.536	0.18	0.99	0.65
Adsorption "A"															
1A1	0	200	0.0002			-0.322	0.037			0.008			0.48	0.98	
1A2	0	400	0.0003							0.018			0.53	0.98	
1A3	0	700	0.0005			-0.296	0.049			0.029			0.52	0.98	
1A4	0	1400	0.0011							0.046			0.56	0.98	
1A5	0	2500	0.0020			-0.297	0.044			0.169			0.59	0.99	
1A6	0	4000	0.0028							0.260			0.49	0.99	

Table 1 continued

	Initial fluid					Solids				Fluids					
Sample ID	**Si initial**	**Ni initial**	**Ni/Fe**	**Ni/Si**	**Si/Fe**	**δ^{60}Ni**	**2se**	**δ^{30}Si**	**2σ**	**Ni/Fe**	**Ni/Si**	**Si/Fe**	**F^{Ni}_{Solid}**	**F^{Fe}_{Solid}**	**F^{Si}_{Solid}**
	mM	*nM*	*mol/mol*	*mol/mol*	*mol/mol*	*‰*	*‰*	*‰*	*‰*	*mol/mol*	*mol/mol*	*mol/mol*			
Adsorption "A" Continued															
1A19	0.67	200	0.0001	0.0006	0.14					0.065	0.000	0.065	0.30	1.00	0.13
1A20	0.67	400	0.0003	0.0019	0.15					0.191	0.000	0.191	0.58	1.00	0.15
1A21	0.67	700	0.0003	0.0017	0.19					0.217	0.001	0.217	0.33	1.00	0.19
1A22	0.67	1400	0.0006	0.0027	0.23					0.196	0.002	0.196	0.32	0.99	0.25
1A23	0.67	2500	0.0010	0.0039	0.26					0.189	0.004	0.189	0.28	0.99	0.27
1A24	0.67	4000	0.0016	0.0049	0.33					0.115	0.007	0.115	0.28	0.97	0.35
1A7	1.1	200	0.0001	0.0006	0.17					0.081	0.000	0.081	0.37	1.00	0.10
1A8	1.1	400	0.0001	0.0006	0.20					0.413	0.000	0.413	0.19	1.00	0.11
1A9	1.1	700	0.0002	0.0009	0.23					0.206	0.001	0.206	0.18	1.00	0.14
1A10	1.1	1400	0.0004	0.0019	0.23					0.122	0.001	0.122	0.19	0.99	0.13
1A11	1.1	2500	0.0008	0.0027	0.28					0.073	0.002	0.073	0.19	0.96	0.16
1A12	1.1	4000	0.0011	0.0033	0.34					0.117	0.004	0.117	0.17	0.95	0.19
1A13	2.2	200	0.0005	0.0020	0.24	-0.376	0.028	-2.11	0.06	0.076	0.000	0.076	0.77	1.00	0.08
1A14	2.2	400	0.0002	0.0007	0.27			-1.60	0.08	0.134	0.000	0.134	0.35	1.00	0.08
1A15	2.2	700	0.0002	0.0008	0.28	-0.717	0.024	0.56	0.10	0.325	0.000	0.325	0.19	1.00	0.08
1A16	2.2	1400	0.0003	0.0010	0.32			0.25	0.11	0.132	0.001	0.132	0.14	0.99	0.10
1A17	2.2	2500	0.0006	0.0017	0.36	-0.862	0.021			0.069	0.001	0.069	0.15	0.95	0.11
1A18	2.2	4000	0.0008	0.0023	0.36			0.34	0.07	0.040	0.002	0.040	0.11	0.86	0.11
Adsorption "B"															
1B19	0.67	200	0.0001	0.0001	0.69					0.015	0.000	0.015	0.34	0.99	0.44
1B20	0.67	400	0.0001	0.0002	0.70					0.028	0.000	0.028	0.26	0.99	0.47
1B21	0.67	700	0.0003	0.0004	0.77					0.022	0.001	0.022	0.26	0.97	0.48
1B22	0.67	1400	0.0006	0.0007	0.87					0.290	0.002	0.290	0.31	1.00	0.56
1B23	0.67	2500	0.0010	0.0010	0.99					1.395	0.004	1.395	0.30	1.00	0.61
1B24	0.67	4000	0.0015	0.0021	0.73					7.166	0.004	7.166	0.26	1.00	0.43
1B7	1.1	200	0.0001	0.0001	0.88					0.005	0.000	0.005	0.28	0.95	0.33
1B8	1.1	400	0.0001	0.0001	1.08					0.011	0.000	0.011	0.15	0.94	0.36
1B9	1.1	700	0.0002	0.0003	0.84					0.012	0.001	0.012	0.17	0.91	0.33
1B10	1.1	1400	0.0006	0.0004	1.27					0.026	0.001	0.026	0.22	0.93	0.47
1B11	1.1	2500	0.0010	0.0009	1.06					0.121	0.003	0.121	0.21	0.97	0.45
1B12	1.1	4000	0.0015	0.0012	1.26					1.528	0.006	1.528	0.19	1.00	0.53
1B13	2.2	200	0.0001	0.0001	1.28	-0.315	0.028	0.16	0.05	0.004	0.000	0.004	0.29	0.94	0.27
1B14	2.2	400	0.0002	0.0001	1.61	-0.424	0.025	-0.57	0.07	0.004	0.000	0.004	0.21	0.85	0.29
1B15	2.2	700	0.0003	0.0002	1.67	-0.580	0.024	-0.07	0.05	0.004	0.000	0.004	0.14	0.71	0.27
1B16	2.2	1400	0.0005	0.0002	2.18			-0.95	0.03	0.004	0.001	0.004	0.10	0.48	0.26
1B17	2.2	2500	0.0009	0.0005	1.64	-0.586	0.017	-0.01	0.07	0.007	0.001	0.007	0.04	0.24	0.09
1B18	2.2	4000	0.0017	0.0006	2.78			0.22	0.05	0.009	0.002	0.009	0.10	0.36	0.28

Table 2 – Chemical data for ferrihydrite solids and experimental fluids from Experiment 2, 3 and 4

	Initial fluid			Solids							Fluids					
Sample ID	**Si initial**	**Ni initial**	**pH**	**Ni/Fe**	**Ni/Si**	**Si/Fe**	**δ^{60}Ni**	**2se**	**δ^{30}Si**	**2σ**	**Ni/Fe**	**Ni/Si**	**Si/Fe**	**F^{Ni}_{Solid}**	**F^{Fe}_{Solid}**	**F^{Si}_{Solid}**
	mM	*nM*		*mol/mol*	*mol/mol*	*mol/mol*	*‰*	*‰*	*‰*	*‰*	*mol/mol*	*mol/mol*	*mol/mol*			
Coprecipitation																
3C3	2.2	2500	4	0.0002	0.0001	2.10			0.58	0.08	0.003	0.002	0.003	0.01	0.07	0.07
3C4	2.2	2500	5	0.0003	0.0002	1.12			0.70	0.03	0.005	0.002	0.005	0.03	0.35	0.20
3C5	2.2	2500	6	0.0005	0.0003	1.73			0.85	0.05	0.034	0.004	0.034	0.12	0.90	0.62
2C1	2.2	2500	7	0.0021	0.0014	1.45	-0.344	0.038	0.39	0.27	0.036	0.001	0.036	0.67	0.97	0.56
2C2	2.2	2500	7	0.0011	0.0008	1.34	-0.328	0.042	0.56	0.08	0.532	0.002	0.532	0.28	0.99	0.53
2C3	2.2	2500	7	0.0011	0.0008	1.42	-0.323	0.049	0.62	0.24	0.568	0.002	0.568	0.29	1.00	0.54
2C4	2.2	2500	7	0.0011	0.0007	1.49	-0.380	0.044	0.35	0.09	0.295	0.002	0.295	0.28	0.99	0.54
2C5	2.2	2500	7	0.0011	0.0008	1.44	-0.352	0.039	0.26	0.21	0.314	0.002	0.314	0.28	0.99	0.52
2C6	2.2	2500	7	0.0010	0.0007	1.43	-0.339	0.048	-0.03	0.19	0.410	0.002	0.410	0.25	0.99	0.49
2C7	2.2	2500	7	0.0011	0.0007	1.47			0.23	0.28	0.371	0.002	0.371	0.26	0.99	0.49
2C8	2.2	2500	7	0.0011	0.0007	1.49	-0.354	0.051	0.43	0.07	0.407	0.002	0.407	0.29	0.99	0.54
2C9	2.2	2500	7	0.0011	0.0007	1.49			-0.33	0.09	0.446	0.002	0.446	0.28	0.99	0.52
2C10	2.2	2500	7	0.0011	0.0007	1.46	-0.304	0.038	-0.43	0.09	0.421	0.002	0.421	0.29	0.99	0.54
2C11	2.2	2500	7	0.0011	0.0007	1.55	-0.343	0.041	-0.62	0.10	0.246	0.002	0.246	0.31	0.99	0.57
Coprecipitation																
4C7	0	2500	4	0.0006							0.006			0.10	0.51	
4C8	0	2500	5	0.0008							0.010			0.17	0.70	
4C9	0	2500	6	0.0011							0.044			0.30	0.94	
4C10	0	2500	7	0.0019							0.103			0.62	0.99	
4C11	0	2500	8	0.0026							0.020			0.94	0.99	
4C12	0	2500	9	0.0026							0.008			0.97	0.99	
4C13	1.1	2500	4	0.0004	0.0004	0.93					0.003	0.003	0.003	0.03	0.20	0.18
4C14	1.1	2500	5	0.0004	0.0004	0.99					0.006	0.006	0.006	0.04	0.39	0.38
4C15	1.1	2500	6	0.0005	0.0006	0.83					0.009	0.006	0.009	0.09	0.62	0.48
4C16	1.1	2500	7	0.0012	0.0015	0.81					1.892	0.006	1.892	0.29	1.00	0.65
4C17	1.1	2500	8	0.0022	0.0026	0.86					1.129	0.002	1.129	0.68	1.00	0.65
4C18	1.1	2500	9	0.0026	0.0034	0.75					0.569	0.001	0.569	0.77	1.00	0.57
4C1	2.2	2500	4													
4C2	2.2	2500	5	0.0003	0.0003	1.16			0.47	0.10	0.006	0.002	0.006	0.04	0.47	0.35
4C3	2.2	2500	6	0.0003	0.0003	1.21			0.68	0.01	0.006	0.001	0.006	0.02	0.23	0.13
4C4	2.2	2500	7	0.0010	0.0013	0.75			0.16	0.07	0.621	0.001	0.621	0.30	1.00	0.42
4C5	2.2	2500	8	0.0021	0.0023	0.89			0.37	0.06	0.262	0.000	0.262	0.74	1.00	0.52
4C6	2.2	2500	9	0.0025	0.0025	0.98			-0.44	0.08	0.189	0.001	0.189	0.89	1.00	0.54

Table 2 continued

Initial fluid				Solids							Fluids					
Sample ID	**Si initial**	**Ni initial**	**pH**	**Ni/Fe**	**Ni/Si**	**Si/Fe**	**δ^{60}Ni**	**2se**	**δ^{30}Si**	**2σ**	**Ni/Fe**	**Ni/Si**	**Si/Fe**	**F^{Ni}_{Solid}**	**F^{Fe}_{Solid}**	**F^{Si}_{Solid}**
	mM	*nM*		*mol/mol*	*mol/mol*	*mol/mol*	*‰*	*‰*	*‰*	*‰*	*mol/mol*	*mol/mol*	*mol/mol*			
Adsorption "A"																
4A7	0	2500	4	0.0003							0.352			0.09	0.99	
4A8	0	2500	5	0.0006							0.261			0.14	0.99	
4A9	0	2500	6	0.0008							0.311			0.19	0.99	
4A10	0	2500	7	0.0017							0.127			0.47	0.99	
4A11	0	2500	8	0.0027							0.027			0.93	0.99	
4A12	0	2500	9	0.0029							0.016			0.98	1.00	
4A13	1.1	2500	4	0.0000	0.0001	0.20					0.259	0.004	0.259	0.00	0.99	0.17
4A14	1.1	2500	5	0.0000	0.0001	0.26					0.206	0.003	0.206	0.01	0.98	0.17
4A15	1.1	2500	6	0.0001	0.0005	0.26					0.465	0.003	0.465	0.04	0.99	0.20
4A16	1.1	2500	7	0.0004	0.0016	0.25					0.246	0.003	0.246	0.10	0.99	0.17
4A17	1.1	2500	8	0.0019	0.0080	0.24					0.055	0.001	0.055	0.56	0.97	0.15
4A18	1.1	2500	9	0.0026	0.0101	0.26					0.013	0.000	0.013	0.94	0.99	0.17
4A1	2.2	2500	4													
4A2	2.2	2500	5	0.0001	0.0004	0.13					1.397	0.000	1.397	0.02	1.00	0.06
4A4	2.2	2500	6	0.0002	0.0011	0.15					0.564	0.000	0.564	0.05	0.99	0.07
4A3	2.2	2500	7	0.0005	0.0035	0.15					0.677	0.000	0.677	0.16	1.00	0.07
4A5	2.2	2500	8	0.0017	0.0095	0.18					0.261	0.000	0.261	0.55	0.99	0.08
4A6	2.2	2500	9	0.0026	0.0115	0.23					0.035	0.000	0.035	0.92	0.99	0.08
Adsorption "B"																
4B13	1.1	2500	4	0.0001	0.0001	0.82					0.025	0.003	0.025	0.01	0.56	0.12
4B14	1.1	2500	5	0.0001	0.0001	0.96					0.295	0.004	0.295	0.01	0.96	0.22
4B16	1.1	2500	6	0.0002	0.0004	0.48					0.105	0.004	0.105	0.05	0.97	0.31
4B15	1.1	2500	7	0.0007	0.0009	0.72					3.345	0.002	3.345	0.19	1.00	0.36
4B17	1.1	2500	8	0.0020	0.0022	0.94					0.152	0.001	0.152	0.67	0.99	0.49
4B18	1.1	2500	9	0.0026	0.0028	0.90					0.089	0.000	0.089	0.90	1.00	0.48
4B1	2.2	2500	4													
4B2	2.2	2500	5	0.0001	0.0001	1.32					0.362	0.000	0.362	0.03	0.99	0.36
4B3	2.2	2500	6	0.0002	0.0002	1.25					0.945	0.002	0.945	0.05	1.00	0.32
4B4	2.2	2500	7	0.0005	0.0003	1.74					0.103	0.000	0.103	0.13	0.97	0.43
4B5	2.2	2500	8	0.0020	0.0022	0.92					0.035	0.000	0.035	0.65	0.97	0.28
4B6	2.2	2500	9	0.0027	0.0019	1.42					0.013	0.000	0.013	0.97	0.99	0.40